**Atmospheric
Chemistry
and Physics**

Measured and modelled cloud condensation nuclei number concentration at the high alpine site Jungfraujoch

Z. Jurányi, M. Gysel, E. Weingartner, P. F. DeCarlo, L. Kammermann, and U. Baltensperger

Laboratory of Atmospheric Chemistry, Paul Scherrer Institut, 5232 Villigen PSI, Switzerland

Abstract. Atmospheric aerosol particles are able to act as cloud condensation nuclei (CCN) and are therefore important for the climate and the hydrological cycle, but their properties are not fully understood. Total CCN number concentrations at 10 different supersaturations in the range of $SS = 0.12$–1.18% were measured in May 2008 at the remote high alpine research station, Jungfraujoch, Switzerland (3580 m a.s.l.). In this paper, we present a closure study between measured and predicted CCN number concentrations. CCN predictions were done using dry number size distribution (scanning particle mobility sizer, SMPS) and bulk chemical composition data (aerosol mass spectrometer, AMS, and multi-angle absorption photometer, MAAP) in a simplified Köhler theory. The predicted and the measured CCN number concentrations agree very well and are highly correlated. A sensitivity study showed that the temporal variability of the chemical composition at the Jungfraujoch can be neglected for a reliable CCN prediction, whereas it is important to know the mean chemical composition. The exact bias introduced by using a too low or too high hygroscopicity parameter for CCN prediction was further quantified and shown to be substantial for the lowest supersaturation.

Despite the high average organic mass fraction (∼45%) in the fine mode, there was no indication that the surface tension was substantially reduced at the point of CCN activation. A comparison between hygroscopicity tandem differential mobility analyzer (HTDMA), AMS/MAAP, and CCN derived κ values showed that HTDMA measurements can be used to determine particle hygroscopicity required for CCN predictions if no suitable chemical composition data are available.

Correspondence to: M. Gysel
(martin.gysel@psi.ch)

1 Introduction

In the atmosphere, cloud droplets can form when aerosols are exposed to conditions where the air is supersaturated with water vapour. Those aerosol particles that are able to activate and become cloud droplets are commonly referred to as cloud condensation nuclei (CCN). Changes in the number concentration and properties of atmospheric aerosol particles due to anthropogenic emissions result in increased number concentrations of CCN. This increase of CCN number concentration modifies the microphysical properties of the clouds, thereby causing a radiative forcing (Twomey, 1977; Albrecht, 1989) and influencing our climate (IPCC, 2007).

The critical supersaturation (SS_{crit}), defined as the supersaturation (SS) at which the cloud droplet activation will take place, is mainly determined by the diameter of the particle at the point of the activation. This activation diameter depends on the dry diameter and the water uptake at RH below activation (hygroscopicity) of the aerosol particle (Köhler, 1936). The equilibrium vapour pressure over a curved pure water surface is elevated, which hinders the CCN activation. The process of activation can also be influenced by surface active species reducing the surface tension (Shulman et al., 1996; Shilling et al., 2007; King et al., 2009) and by compounds with limited solubility. The latter phenomenon can result in exotic equilibrium growth curves (Köhler curves) for aerosol mixtures (Petters and Kreidenweis, 2008). The aerosol mixing state (internally or externally mixed) can also play a role in the CCN activation behaviour of an aerosol population.

Ambient aerosols are mainly composed of complex mixtures (e.g. Krivácsy et al., 2001; Shulman et al., 1996). The main components are inorganic ions, organic components, black carbon and mineral dust (Zhang et al., 2007). The hygroscopicity of single component inorganic aerosols is

already well characterised (Clegg et al., 1998; Topping et al., 2005; Petters and Kreidenweis, 2007). Single component and mixed organic aerosols have also been studied many times (e.g. Saxena and Hildemann, 1996) but the properties of these mixtures are less understood. Pure black carbon and mineral dust particles are thought to be much less relevant in CCN activation because they are insoluble and therefore activate at much higher SS_{crit} (Kuwata et al., 2009; Koehler et al., 2009; Herich et al., 2009). Understanding the activation process of ambient aerosols is a big challenge because it is impossible to get size- and mixing state resolved chemical composition data including complete speciation of all organic compounds.

Examination of the aerosol parameters contributing to CCN activity, such as size and chemical composition or hygroscopicity, can be used with the existing cloud droplet activation theories to predict CCN properties and their number concentration for comparison with direct measurements, commonly referred to as CCN closure studies. Such studies provide feedback on how well we understand the activation and water uptake process and to what extent simplifications can be introduced in the models without impairing predictions of CCN number concentrations. Comparison of water uptake on aerosols below saturation with CCN properties using different parameterisations of the Köhler curve is a common type of a closure study (Kammermann et al., 2010a, and references therein), hereafter referred to as hygroscopicity-CCN closure studies.

Composition-CCN closure studies, which link chemical composition and size distribution of the aerosol with CCN properties or number concentrations, are a different approach. Several studies appeared in the literature with different methods how they treat the chemical composition and mixing state and with different closure success. The Aerodyne Aerosol Mass Spectrometer (AMS) is most commonly used in CCN closure studies for measuring the chemical composition (Ervens et al., 2007; Cubison et al., 2008; Lance et al., 2009; Broekhuizen et al., 2006; Stroud et al., 2007) but filter measurements are used as well (Liu et al., 1996; Bougiatioti et al., 2009). Ervens et al. (2007) also tried to reach closure between light scattering enhancement factors and CCN properties.

Numerous simple approaches treat the aerosol composition as a two-component mixture, consisting of a water-soluble inorganic fraction, represented as ammonium sulphate, and a water-insoluble organic fraction (Liu et al., 1996; Gunthe et al., 2009; Broekhuizen et al., 2006). However, several recent studies indicated that a substantial fraction of the organic species is water-soluble, thus also contributing to the reduction of critical supersaturation for CCN activation (e.g. Moore et al., 2008; Vestin et al., 2007). Bougiatioti et al. (2009) found that including the solubility of organics significantly improved the quality of the prediction by lowering the underprediction of CCN concentration from 16% to 0.6% at their lowest measured SS. The two-

component chemical models do not include refractory material such as black carbon, mineral dust, sodium chloride, which is also not measured by the AMS. The potential influence of the insoluble black carbon can be estimated by running a light absorption measurement in parallel to the AMS (Ervens et al., 2010).

The size dependence of the chemical composition and the mixing state – internal versus external mixture – are accounted for in various ways. The simplest approach is to use bulk chemical composition data, which means ignoring the size dependence and assuming internal mixture. Some studies account for the size dependent chemical composition by using size-resolved AMS data (Cubison et al., 2008) or in a simplified form by treating two (or more) size modes with different composition separately (Broekhuizen et al., 2006; Stroud et al., 2007). The common methods for chemical composition measurements do not provide information on the mixing state of the aerosol, however, recent studies by Cubison et al. (2008) and Ervens et al. (2010) tested different assumptions regarding the mixing state of the aerosol. The elemental carbon and/or organic fraction were assumed to be externally mixed with the rest of the aerosol in their calculations. Ervens et al. (2010) compared closure studies from 6 different locations with different distances to the sources. They showed that a fresh pollution aerosol cannot be represented without size resolved chemical composition, but assuming either externally or internally mixed soluble organics leads to similar predictions of CCN number concentrations.

All above-mentioned closure studies approximate the surface tension of the solution (σ_{sol}) at the point of activation by the surface tension of pure water. Lance et al. (2009) did calculations using a surface tension that was 0.015 N/m lower than for pure water (i.e. $\sigma_{sol} \approx 0.8 \times \sigma_{water}$, at a temperature of 20 °C) and concluded that CCN predictions became much worse. The same is true for most hygroscopicity-CCN closure studies, which tend to overpredict rather than underpredict CCN number concentration (Kammermann et al., 2010a).

Looking at the performance of the existing closure studies most of them were able to correctly predict the order of magnitude of the CCN number concentration but for only a few of them the average calculated CCN number concentration was within 30% (e.g. Broekhuizen et al., 2006; Kammermann et al., 2010a) and even less achieved very high correlation coefficients (e.g. Bougiatioti et al., 2009). Overall, it appears that with increasing distance from source regions closure is more easily achieved because the aerosol population becomes more homogeneous, i.e. less size dependent, less variable in time and more internally mixed.

Here we present for the first time a CCN closure study covering a wide range of SS (0.12%–1.18%) from a remote continental measurement site which is most of the time situated in the free troposphere and only sometimes influenced by injections from the planetary boundary layer (Nyeki et al., 1998). Here we show that highly time resolved aerosol

Table 1. The used instrumentation and the measured quantities. For detailed description and for meaning of the abbreviations see text.

Instrument	Manufacturer	Measured property
SMPS	TSI, custom made	Size distribution ($12\,\text{nm} < D < 570\,\text{nm}$)
CPC	TSI	Total particle number concentration
OPC	Grimm	Size distribution ($0.3\,\mu\text{m} < D < 20\,\mu\text{m}$)
AMS	Aerodyne, Tofwerk AG	Chemical composition
MAAP	Thermo ESM Andersen	Black carbon mass concentration
HTDMA	Custom made	Hygroscopicity
CCNC	DMT	CCN number concentration

number size distribution data along with knowledge of the mean chemical composition is sufficient for accurate prediction of CCN number concentrations at all investigated supersaturations. A detailed sensitivity study shows that the variability of chemical composition has little influence on CCN number concentrations, whereas the variability of the aerosol number size distribution has a bigger influence.

2 Method

The Jungfraujoch (JFJ) measurement site is a Global Atmosphere Watch (GAW) station where different aerosol properties have been continuously measured since 1995 (Nyeki et al., 1998; Collaud Coen et al., 2007). The site is situated in the Bernese Alps in Switzerland at 3580 m a.s.l. Because of its altitude and location it is far away from local pollution and therefore considered as a continental background site. The aerosol shows a strong seasonal variability with higher concentrations in summer and lower concentrations in winter. This is due to the fact that in summer the site is influenced by injections from the more polluted planetary boundary layer because of the stronger thermal convection, while during winter the site mostly stays in the undisturbed free troposphere. A more detailed description of the site can be found elsewhere (Baltensperger et al., 1997).

Measurements were conducted during the EUCAARI (European Integrated Project on Aerosol-Cloud-Climate and Air Quality Interactions) intensive campaign in May 2008 (Kulmala et al., 2009). Air was sampled through a heated ($25\,^\circ$C) inlet in order to evaporate any water that is associated with those aerosol particles that formed cloud droplets or ice crystals. The inlet has been designed such that it samples not only the interstitial aerosols but also the cloud droplets and ice crystals up to 40 μm. A detailed description of this "total aerosol inlet" is given elsewhere (Weingartner et al., 1999; Henning et al., 2002). Heating the aerosol from $\sim -4.5\,^\circ$C (mean outdoor temperature in May 2008) to $\sim 25\,^\circ$C lab temperature also dries it to RH $<10\%$. All instruments of which data are used in this manuscript were connected to this inlet and are summarized in Table 1.

The aerosol number size distribution between diameters of 12 and 570 nm was measured with a scanning mobility particle sizer (SMPS). It consisted of a differential mobility analyzer (DMA, TSI 3071) and a condensation particle counter (CPC, TSI 3772). The size distribution was measured every 6 min, with an up-scan time of 300 s. The DMA was operated with $1\,\text{L}\,\text{min}^{-1}$ sample air flow rate and a closed-loop sheath air flow rate of $5\,\text{L}\,\text{min}^{-1}$. The sheath flow rate was continuously regulated to a constant volumetric flow, using a mass flow controller with continuously pressure and temperature compensated mass flow set point. All flow rates were regularly checked with a bubble flowmeter. Sizing accuracy was checked by using polystyrene latex (PSL) spheres of different diameters. The peak position agreed within $\pm 3\%$ with the nominal size of the certified PSL spheres, which is within uncertainty. An identical copy of this SMPS instrument participated in the EUSAAR SMPS intercomparison workshop in 2008 in Leipzig.

The total number particles with diameter larger than 10 nm (N_{CN}) was also monitored by a CPC (TSI 3010). A comparison of the integrated SMPS concentration (N_{12-570}) with the CPC data revealed that the SMPS number concentration data had to be corrected by a factor of 1.2 (see details in the Appendix). Undercounting of the SMPS was confirmed by further instrument comparisons and may have been caused by slight deviations of the sample and sheath flow rates from the nominal values, or a DMA transfer probability which was lower than assumed.

In addition to the SMPS, an optical particle counter (OPC, Grimm Dustmonitor 1.108) was used to measure the size distribution of the larger particles in the optical diameter range $0.3\,\mu\text{m}$ to $20\,\mu\text{m}$. In this instrument particles are illuminated by a laser beam, and the scattered light is used to determine their optical size.

An Aerodyne high resolution time-of-flight aerosol mass spectrometer (AMS) was used to measure the size resolved aerosol chemical composition of the non-refractory submicron aerosol particles (DeCarlo et al., 2006; Canagaratna et al., 2007). The aerosol is sampled through an aerodynamic lens which focuses particles between 35 nm and $1.5\,\mu\text{m}$ into a tight beam. After the time of flight sizing the particles impact on an inverted conical tungsten

vapour, where the non-refractory components are flash vapour. The resulting gas is then ionised by electron ionisation at 70 eV. A high mass resolution mass spectrometer (H-TOF, Tofwerk AG, Thun, Switzerland) produces a time series of mass spectra which is processed using custom software (http://cires.colorado.edu/jimenez-group/ToFAMSResources/ToFSoftware/index.html) to give mass concentrations of non-refractory species. The collection efficiency as determined by intercomparison with other collocated instruments (e.g. SMPS and nephelometer) was found to be 1 at the JFJ for the deployed instrument. The measured ionic species account for 96% of the total ionic mass at the measurement site (Cozic et al., 2008; Henning et al., 2003), thus the refractory ionic species can be neglected.

The AMS does not detect refractory material such as black carbon (BC), therefore a multi-angle absorption photometer (MAAP, Thermo ESM Andersen) operating at a wavelength of 630 nm (Petzold and Schonlinner, 2004) was used to measure the BC mass concentration during the measurement campaign. The MAAP is part of the continuous measurement program of GAW. The absorption values were converted into BC mass concentration using a mass absorption efficiency of $6.6 \, \text{m}^2 \, \text{g}^{-1}$ (Petzold et al., 2005).

Mineral dust is another type of refractory material that is not detected by the AMS. The contribution of this material to the total aerosol number concentration is normally low at our measurement site, though the contribution to the total mass is considerable during Saharan dust events (SDE). The potential influence of neglecting the mineral dust in our CCN predictions is discussed in Sect. 4.8.

A custom built hygroscopicity tandem differential mobility analyzer (HTDMA) based on the instrument presented by Weingartner et al. (2002), was operated to measure the hygroscopic growth factor GF at a constant relative humidity (RH) of 90% of six different dry diameters (D_0=35, 50, 75, 110, 165 and 265 nm). The instrument was designed such that the residence time between the DMAs was ~20 s; sufficient for most atmospheric aerosols to reach equilibrium at high RH (Sjogren et al., 2007). The HTDMA raw data were corrected against dry GF-offsets by linearly interpolating deviations between two validation sessions, and inverted using the TDMAinv algorithm by Gysel et al. (2009). Only HTDMA data measured at an RH within the range 88%<RH<92% were used to derive the hygroscopicity parameter κ (Petters and Kreidenweis, 2007).

A single-column continuous-flow streamwise thermal-gradient CCN chamber (DMT CCNC-100, Roberts and Nenes, 2005) was used to measure the total polydisperse CCN number concentration as a function of time and supersaturation (SS). The latter is determined by the temperature gradient applied along the wetted wall of the column, where the activation takes place. The particles that have lower SS_{crit} than the SS in the column will activate and grow into the supermicron size-range. Particles leaving the column are sized by an optical particle counter (OPC) and counted as CCNs

if their diameter is larger then a threshold size of typically 1 μm.

The CCNC was calibrated regularly by using nebulised, size selected (with the DMA) ammonium sulphate particles (Rose et al., 2008). At a certain temperature gradient the DMA size was stepped (D-scans) and the critical dry diameter ($D_{0,\text{crit}}$), where 50% of the singly charged ammonium sulphate particles were activated, was determined by fitting the sum of two sigmoid functions – in order to account for doubly charged particles – to the activation curve. The SS_{crit} corresponding to $D_{0,\text{crit}}$ was obtained from the ADDEM model (Topping et al., 2005). During calibrations 10 different temperature gradients were set in the CCNC such that the resulting SS values covered the range of SS=0.07–1.1%. The calibration curve was linear and remained stable during the measurement campaign (SS = 0.097% $K^{-1} \cdot \Delta T$ − 0.139%, where ΔT is the temperature difference over the column).

The CCNC was operated at a total flow rate of $1 \, \text{L} \, \text{min}^{-1}$ with a sheath-to-aerosol flow ratio of 10. One measurement cycle included measurements at 10 different SS (0.12%–1.18%). The CCN concentration at each SS was measured for 3 min, which adds up to a total time of 50–60 min for the complete cycle including the time required for SS stabilisation at each setpoint.

3 Theory

A particle's ability to act as CCN depends on its chemical composition and size. Both chemical composition and particle number size distribution data are available in this study, which makes an independent calculation of the expected CCN number concentration at a given supersaturation possible. For this purpose the critical dry diameter for CCN activation at a given supersaturation was calculated from the composition data using a simplified Köhler theory.

The equilibrium saturation ratio $S=p/p_0$, where p is the partial vapour pressure of water and p_0 is the saturation vapour pressure of water, over an aqueous solution droplet can be described by the Köhler theory (Köhler, 1936; Mc-Figgans et al., 2006):

$$S = a_w \exp\left(\frac{4\sigma_{\text{sol}}\nu_w}{RT D_{\text{drop}}}\right) \tag{1}$$

where a_w is the water activity of the solution, σ_{sol} is the surface tension of the solution, ν_w is the partial molar volume of water in solution, R is the universal gas constant, T is the temperature and D_{drop} is the droplet diameter.

We used a semi-empirical water activity parameterisation, which was introduced by Petters and Kreidenweis (2007):

$$a_w = \left(1 + \kappa \frac{D_0^3}{D_{\text{drop}}^3 - D_0^3}\right)^{-1} \tag{2}$$

Table 2. The chemical species, their densities and their κ values that were used for our model calculations.

Component	Density [kgm^{-3}]	κ_i [–]
Black carbon	1770 (Park et al., 2004)	0 (Weingartner et al., 1997)
Organics	1270 (Cross et al., 2007)	0.1 (Sjogren et al., 2008; Jurándyi et al., 2009)
(NH$_4$)$_2$SO$_4$	1769	0.61 (Petters and Kreidenweis, 2007)
NH$_4$NO$_3$	1720	0.67 (Petters and Kreidenweis, 2007)

where κ is the hygroscopicity parameter, and D_0 the dry particle diameter. Substituting a_w in Eq. (1) with Eq. (2) provides the κ-Köhler equation:

$$S = \left(1 + \kappa \frac{D_0^3}{D_{\text{drop}}^3 - D_0^3}\right)^{-1} \exp\left(\frac{4\sigma_{\text{sol}} v_w}{RT D_{\text{drop}}}\right) \quad (3)$$

The SS_{crit} of a particle with known properties (D_0, κ, σ_{sol}) corresponds to the maximum of Eq. (3) with D_{drop} as the independent variable. The critical dry diameter of a particle, $D_{0,\text{crit}}$, with known properties (κ, σ_{sol}) and at a given SS is also obtained through Eq. (3) by varying D_0 until the corresponding SS_{crit} becomes equal to the given SS.

The κ parameter of a mixture of n different compounds (or compound classes) is the linear combination of the individual κ_i in pure form weighted by their respective volume fractions, ϵ_i, in the mixed, dry particle:

$$\kappa = \sum_{i=1}^{n} \epsilon_i \kappa_i \quad (4)$$

This equation is equivalent to the Zdanovskii-Stokes-Robinson (ZSR) mixing rule (Stokes and Robinson, 1966).

The volume fractions ϵ_i of the individual components were calculated from the measured mass concentrations, m_i, and their respective densities, ρ_i:

$$\epsilon_i = \frac{m_i/\rho_i}{\sum m_k/\rho_k} \quad (5)$$

The κ values of ambient aerosol compounds vary between 0 (insoluble, wettable) and ~ 1.2–1.33 (pure NaCl). Table 2 summarizes the individual species and compound classes along with their properties (κ_i, ρ_i) that were used in our calculation. Here we use constant κ_i values, setting aside that κ_i at the point of CCN activation may vary with the dry diameter (e.g. for pure ammonium sulphate $\kappa = 0.59$ for $D_0 = 50$ nm and $\kappa = 0.65$ for $D_0 = 150$ nm).

The composition-derived κ parameter of the mixed atmospheric aerosol was calculated using Eqs. (4) and (5), thereby assuming an internally mixed aerosol and size-independent chemical composition. Justification of the latter assumption is discussed in Sect. 4.2. Using this composition-derived and time-dependent κ along with Eq. (3) makes it possible to calculate for the SS set in the CCNC the critical diameter ($D_{0,\text{crit}}$). All particles larger than $D_{0,\text{crit}}$ will activate as

CCN, assuming internal mixture. Integrating the size distribution provided by the SMPS from $D_{0,\text{crit}}$ up to the largest measured size then gives the predicted CCN number concentration.

We assumed surface tension of pure water in our calculations, even though surface active organic compounds have the potential to lower the surface tension. Potential effects of this assumption are discussed in Sect. 4.5.

4 Results and discussion

4.1 Measured aerosol properties

All extensive aerosol properties show a strong seasonal variability at the JFJ, with much higher values in summer than in winter (Collaud Coen et al., 2007). From this perspective the month May can be described as an intermediate month with episodes of both undisturbed free tropospheric conditions as well as influence by injections from the planetary boundary layer.

For our CCN closure experiment we measured the following aerosol properties throughout May 2008: CCN number concentration at different supersaturations as well as dry particle number size distribution and chemical composition. Time series of these measurements are shown in Figs. 1–3. Two distinct synoptic conditions were encountered during the measurement period. In the first half and at the very end of the campaign the aerosol number, CCN and mass concentrations were relatively high, indicating influence of boundary layer injections. Much lower concentrations were observed from 16 to 27 May indicating free tropospheric conditions.

The time series of CCN number concentrations measured at different SS is shown in Fig. 1a. CCN number concentrations varied between 0.1 and 600 cm^{-3} at $SS = 0.12\%$ (lowest SS) and between 27 and 1582 cm^{-3} at $SS = 1.18\%$ (highest SS) with mean values and standard deviations of 149 ± 171 cm^{-3} and 568 ± 401 cm^{-3}, respectively. Minimum and maximum observed CCN number concentrations at a certain SS differed by more than two orders of magnitude. Figure 1b shows the activated fraction (AF), defined as the ratio of the CCN number concentration (Fig. 1a) to the integrated SMPS number concentration (Fig. 2a). The activated fraction varied by less than a factor of ~ 4, indicating that
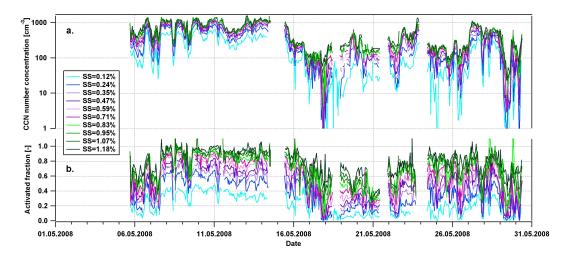
Fig. 1. Time series of **(a)** CCN number concentration (note logarithmic ordinate scale) and **(b)** activated fraction (#CCN/N_{12-570}). The different colours represent the different supersaturations (*SS*).
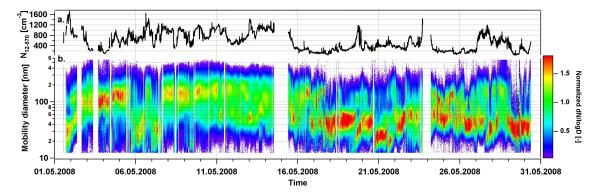

Fig. 2. Size distribution and the integrated number concentration during the measurement campaign. The size distribution was measured by the SMPS between 12 nm and 570 nm mobility diameter and normalized with the integrated number concentration.

most of the high variability of CCN number concentration is due to the variability of the total particle number concentration, while a smaller part of it can be attributed to variations of the aerosol properties such as shape of the size distribution and chemical composition.

Some correlation between the CCN number concentration and the activated fraction was observed for this data set (Fig. 1). Whether this is generally the case will be addressed in a forthcoming manuscript using a separate long-term data set.

In May 2008, the aerosol number size distribution (Fig. 2b, normalised with the integrated concentration) was most of the time monomodal, occasionally bimodal. The geometric mean diameter varied between 28 and 120 nm with a mean value of 71 nm and the integrated number concentration varied between 40 and 1720 cm^{-3} with a mean value of 550 cm^{-3}. Please note, that the average CCN number concentration at $SS=1.18\%$ exceeds the average integrated number concentration, this is due to the different time periods over which the averaging was done. A trend towards slightly

bigger particle size during the period with influence from the planetary boundary layer compared to the free tropospheric conditions was observed. This is in line with the findings previously reported by Weingartner et al. (1999) based on a whole year of size distribution measurements.

During nucleation events a substantial fraction of the aerosols was possibly present below 12 nm and was therefore not measured by the SMPS. However this does not affect our calculated CCN number concentration because $D_{0,\text{crit}}$ at the highest *SS* was on average at 31 nm and always above 27 nm. On the other hand, the aerosol particles with diameters larger than 570 nm are not captured either by the SMPS. These large particles will always act as CCN due to their large dry size, even if they are just slightly hygroscopic (minimum required $\kappa = 0.005$ at $SS = 0.12\%$ for a 570-nm particle). However, the OPC measurements show that the number concentration of particles above the upper detection limit of the SMPS is always negligible compared to the number concentration of CCN, even at the lowest applied *SS*.
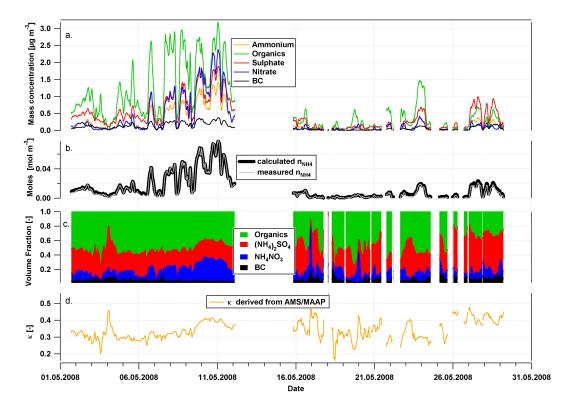
Fig. 3. Chemical composition of the aerosol, measured by the AMS and the MAAP. **(a)** shows the mass concentration of the individual species using a collection efficiency of 1 in the AMS. **(b)** shows the molar concentration of the measured NH_4 and the amount that is needed for complete neutralization. On **(c)** the volume fractions of the organics, NH_4NO_3, $(NH_4)_2SO_4$ and black carbon are shown; the calculation was done using the density values of $1270\,kg/m^3$, $1720\,kg/m^3$, $1769\,kg/m^3$ and $1770\,kg/m^3$, respectively. **(d)** shows the hygroscopicity parameter κ which was calculated from the volume fraction weighted sum of the κ_i values of the above species.

The bulk mass concentrations of ammonium, sulphate, nitrate and organics as measured by the AMS, are shown in Fig. 3a, along with the BC mass concentrations measured by the MAAP. Due to the low aerosol mass concentrations of the measured species (the mean total mass concentration was $1.93\,\mu g\,m^{-3}$) averaging to a 2-h running mean was necessary. No substantial size dependence of the chemical composition was observed in the time-averaged AMS data (see also Sect. 4.2). The charge balance based on the ammonium, nitrate and sulphate concentrations revealed that the aerosol was completely neutralised within the detection limits of the AMS (Fig. 3b). Therefore these ions can be paired to NH_4NO_3 and $(NH_4)_2SO_4$ for the ZSR calculations.

Figure 3c shows the volume fractions of the chemical components, which were calculated from the respective mass fractions using Eq. (5) and the densities listed in Table 2. The average values of the observed volume fractions were: 5.7%, 13.3%, 33.3%, 47.7% for BC, NH_4NO_3, $(NH_4)_2SO_4$ and organics, respectively. Similar values were found during previous measurement campaigns at the same measurement site during February and March in 2005 (3.8%, 9.0%, 37.2%, 50.0%) and during July and August in 2005 (2.7%, 6.2%, 30.5%, 60.7%) by Cozic et al. (2008), though in May

2008 the organic volume fraction was slightly lower and the NH_4NO_3 slightly higher. The time resolved volume fractions are fed into Eq. (4) to get the AMS/MAAP derived κ as a function of time (Fig. 3d).

The relative contributions of NH_4NO_3 and $(NH_4)_2SO_4$ to the total inorganic volume fraction were changing significantly during the measurement period, whereas the inorganic to organic ratio exhibited much less variability. Since the κ_i values of the different inorganic salts are similar, the overall κ value does not experience large variations either (Fig. 3d). The campaign mean AMS/MAAP derived κ value was 0.34. This value is well representative for the global mean κ values for continental regions (0.27 ± 0.21) whereas the mean value for marine regions (0.72 ± 0.24) is much higher (Andreae and Rosenfeld, 2008; Pringle et al., 2010).

4.2 Applicability of using AMS bulk composition data

Using bulk instead of size resolved chemical composition data does not introduce significant prediction bias for the following reasons:

1. The applicability of this simplification was confirmed by checking the size dependent AMS signal.
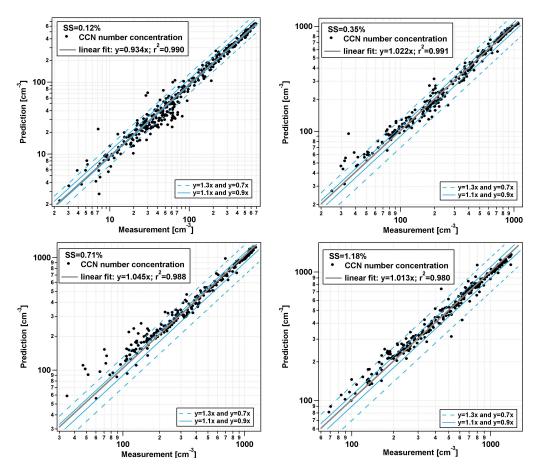
Fig. 4. Predicted vs. measured CCN number concentration for ambient aerosol at 4 different supersaturations using size distribution and chemical composition data. The grey line shows the fitted line through the data points. The method of the fit is explained in the text in details. The blue lines obey the $y = 1.3x, 1.1x, 0.9x, 0.7x$ equations.

Throughout the diameter range of our interest only a very slight size dependence can be seen on average, and because of the very low mass concentrations at JFJ, the use of size dependent data would introduce much more noise than add true information on the size dependence of the composition.

2. The HTDMA measurements corroborate the fact that the κ values show almost no size dependence at the Jungfraujoch (Kammermann et al., 2010b). The same measurements also showed that the aerosol is largely internally mixed with respect to hygroscopicity most of the time. Moreover, Ervens et al. (2010) also showed that assuming the two extreme cases – completely internally or externally mixed aerosols – does not result in a significant difference in the predicted CCN number concentration.

The chemical composition around $D_{0,\mathrm{crit}}(SS)$ is relevant for determining the CCN activation cut-off. The highest $D_{0,\mathrm{crit}}$ values belong to the lowest supersaturations. The AMS integrates all the mass below 1.5 μm in diameter (vac-

uum aerodynamic diameter), therefore larger accumulation mode particles, carrying much more mass per particle, will mainly determine the measured chemical composition. For this reason, the measured chemical composition is biased towards larger diameters and with that it is most representative for low supersaturations. Fortunately CCN predictions are most sensitive to changes in the hygroscopicity parameter κ at low supersaturations, while the susceptibility to κ is small at medium and high supersaturations (see Sect. 4.6 for details).

4.3 CCN prediction from chemical composition data

Correlations between predicted and measured CCN number concentrations on log-log scale at 4 example supersaturations (0.12%, 0.35%, 0.71% and 1.18%) are shown in Fig. 4. The solid and dashed blue lines represent agreement within ±10% and ±30%, respectively. The orthogonal distance regression line weighted by inverse measurement uncertainties and forced through the origin is shown in grey. We associated 5% relative error to the measured and 10% to the predicted CCN number concentration.

Table 3. Details on the predicted vs. measured CCN number concentration for the CCN prediction without simplifications. a is the slope of the fitted line, R^2 is the square of the correlation coefficient.

SS [%]	a [–]	R^2 [–]
0.12	0.934	0.990
0.24	1.028	0.992
0.35	1.022	0.991
0.47	1.042	0.987
0.59	1.045	0.987
0.71	1.045	0.988
0.83	1.032	0.987
0.95	1.049	0.979
1.07	1.050	0.978
1.18	1.013	0.980

At every single SS the slope of the fitted line is close to 1 which means that the CCN closure was successful (see Table 3 for results at all SS). On average 104% of the measured CCN concentration was predicted across all SS, with the highest value of 105.0% at $SS = 1.07$% and the lowest value of 93.4% at $SS = 0.12$%. Overall, a very slight overprediction can be seen (except for the lowest SS), however, the deviations are clearly within the experimental uncertainty. At high CCN number concentrations most of the points are within the 10% and virtually all points within the 30% limits, while at lower number concentrations (#CCN<100–200 cm^{-3}, depending on which SS one looks at) the scatter of individual data points increases slightly with a few of them exceeding the 30% limit (see Fig. 5). The reason for this could be the overall increased uncertainty of the measurements closer to the detection limits of the instruments. Next to this most of the predictions outside the 30% limit belong to times when the mean diameter of the size distribution is very low (Fig. 5). This means that only the tail of the size distribution was integrated for the CCN prediction, where even a small absolute noise of the SMPS can cause relatively high prediction errors.

CCN predictions of our closure study agreed well with measured values for every single data point, which is reflected in a fitted slope of nearly unity as well as a high correlation coefficient ($R^2 > 0.97$) between the two quantities. In a different CCN closure study Lance et al. (2009) reported agreement between prediction and measurement on average (fitted slope near unity), whereas the disagreement for individual data points was considerable (small correlation coefficient). The improved performance of our closure study is likely due to the fact that the number size distribution and chemical composition are more stable for the remote JFJ aerosol, which is not influenced by local pollution in contrast to measurements performed in the planetary boundary layer. Potential reasons for degrading performance of CCN closure studies conducted at sites closer to sources are: increased
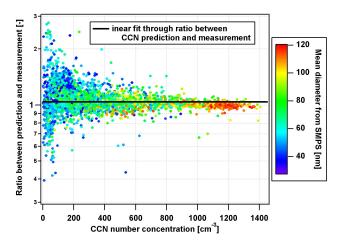

Fig. 5. The predicted-to-measured CCN number concentration at all SS as function of the CCN number concentration coloured after the mean diameter of the number size distribution.

temporal variability of aerosol number concentration, shape of the number size distribution and chemical composition. In addition the assumption of size-independent chemical composition may become invalid (Ervens et al., 2010) and a substantial fraction of externally mixed particles with very low κ values may be present.

4.4 Performance of simplified CCN predictions

The sensitivity of the CCN predictions to the input parameters was tested with different simplifying assumption regarding the number size distribution and chemical composition of the aerosol. The reference CCN prediction, considering all available measurements including their temporal variability, is shown as blue squares in Fig. 6. The green diamonds represent the CCN prediction assuming a constant chemical composition, i.e. mean κ based on the average measured composition during the campaign (~ 0.34). Yellow triangles were calculated by ignoring the variability of the shape of the size distribution by time averaging the normalised SMPS scans. In this case the detailed chemical information was used, and the normalised average size distribution was scaled to the measured total particle number concentration (N_{12-570}). Red points were derived by using the number size distribution averaged over the whole campaign in the model, so that the variability of the predicted points originates only from the changes in the chemical composition.

The simplified CCN predictions show that the CCN number concentrations are most sensitive to the temporal variability of the number size distribution (Fig. 6). Using the constant mean size distribution with considering the variability of chemical composition results in useless predictions (red points in Fig. 6). By contrast, deviations from the average measured chemical composition have little to no impact on the variability in the CCN number concentration (cf. blue
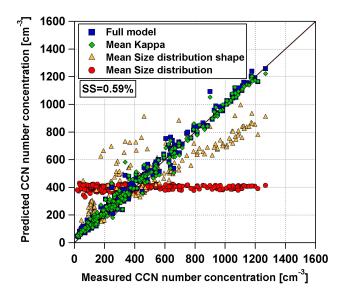
Fig. 6. Predicted vs. measured CCN number concentration for ambient aerosol at SS=0.59% applying different simplifications in the calculation of the predicted CCN number concentration: full model (blue squares), time averaged κ (green diamonds), time averaged size distribution shape (yellow triangles), time averaged number size distribution shape and concentration (red points). The thin black line represents the one-to-one ratio.

squares and green diamonds in Fig. 6). Neglecting only the temporal variability of the size distribution's shape yields still reasonable results (yellow triangles in Fig. 6), however, it has much bigger influence on the prediction's performance than the temporal variability of the chemical composition. Thus, for an aerosol with a relatively constant chemical composition such as at the Jungfraujoch size indeed matters more than chemistry (Dusek et al., 2006), however, this does not necessarily hold for other aerosol types and supersaturations.

The volume fraction of the inorganic compounds ranged from 20% to 80% with the 10th percentile of 37%, median of 45% and 90th percentile of 66% during the one-month observation period. Even though substantial variations in chemical composition were observed, significant differences between the reference prediction and the time averaged κ case cannot be seen. The model performance gets only slightly worse (larger χ^2 values at most of the SS, not shown here) if the time variance of the chemical composition is ignored. Based on this analysis, the temporal variability of the chemical information could be skipped for the calculation, still yielding a reliable CCN prediction at the JFJ.

4.5 Susceptibility to surface tension

Several laboratory studies on organic aerosols indicate that surface tension suppression effects may occur (e.g. Shilling et al., 2007; King et al., 2009). In contrast the results of our closure study give no indication for a suppressed surface ten-

sion of the aerosol at the point of CCN activation. Aerosols with suppressed surface tension activate at lower SS_{crit} because the Kelvin effect term in Eq. (1) is decreased. Assuming a 10% reduction of surface tension at the point of CCN activation relative to pure water increases the predicted CCN number concentration. Consequently the overprediction becomes even higher and reaches a factor of 1.12 averaged over the whole data set compared to a factor of 1.04 with assuming surface tension of pure water. Kammermann et al. (2010a) compiled an overview of the performance of existing hygroscopicity-CCN closure studies, revealing that the CCN number concentration was underpredicted in only 1 out of 10 cases, always assuming surface tension of pure water. This is in line with our result that assuming reduced surface tension impairs the performance of CCN predictions. However, Good et al. (2010a) also reported underprediction of CCN number concentration, which might be an indication for suppressed surface tension in their case.

One has to note that closure with assuming surface tension of pure water might be untruly achieved by compensating errors if both hygroscopicity parameter κ and surface tension are in reality smaller than the values used in the calculations (see also Sect. 4.7). Furthermore, it is also not possible to distinguish between a true absence of surface tension depression and the presence of surface active species compensated by bulk/surface partitioning effects (Sorjamaa et al., 2004) such that one can still assume surface tension of pure water at the point of CCN activation.

4.6 Susceptibility to chemical composition

The susceptibility of CCN predictions to the absolute value and the variability of the chemical composition (κ) was further investigated by a detailed sensitivity analysis. For each SS and each time the relative change in the predicted CCN number concentration at varying κ parameter ($0 < \kappa < 0.8$) was calculated with the help of the measured size distribution. Figure 7 shows one example of the susceptibility to κ for a medium SS of 0.59%. The colour scale indicates relative CCN prediction errors (hereafter referred to as CCNerror) if the κ value shown on the ordinate is used for the prediction instead of the AMS derived κ (grey points). The CCNerror is by definition zero at the grey points. The black lines indicate the lower and upper limits of acceptable κ values for which CCNerror < 10%. The sensitivity of CCN number concentrations is strongly time dependent, reflected in the variability of the equipotential lines of CCN error (see black lines as example). This is mainly caused by the variability of the shape of the size distribution. Nevertheless, a common feature is that CCN number concentrations are generally much more sensitive to a decrease than to an increase in κ, which originates from the nonlinear dependence of $D_{0,\text{crit}}$ on κ.

The mean susceptibility of CCN predictions to the variability of the chemical composition (κ) for all SS is shown in Fig. 8. Note that temporal averaging over the whole
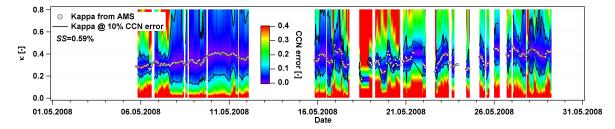
Fig. 7. Sensitivity of the prediction to the κ at 0.59% *SS* as a function of time. The grey dots show the AMS derived κ parameter. The different colours represent the relative change of the predicted CCN concentration as a function of the chosen κ.
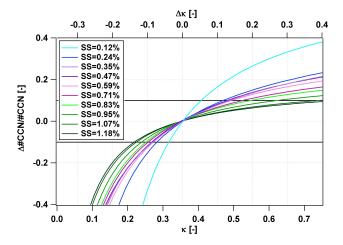

Fig. 8. Time-averaged sensitivity of CCN prediction to changes in assumed κ value. The different colours indicate the different supersaturations.

measurement campaign of the relative prediction error was done against $\Delta\kappa$, and then the $\Delta\kappa$ scale was converted back to absolute κ values using the campaign mean κ of ∼0.34. CCN number concentrations at the lowest investigated *SS* (0.12%) are much more sensitive to the chemical composition change than at any higher *SS*. At this lowest *SS* κ can only vary by −11% to +15% to stay within 10% in the calculated CCN number concentration. The corresponding tolerance for κ at the second lowest *SS* (0.24%) is already −20% to +32%, increasing up to −37% to +120% at the highest *SS* (1.18%). A priori one would expect a symmetrically mirrored order of the sensitivity curves at different *SS* for positive and negative $\Delta\kappa$, i.e. the curves shown in Fig. 9 are expected to cross each other at $\Delta\kappa = 0$ and nowhere else. This is the case for most pairs of sensitivity curves. However, the sensitivity to κ for nearby supersaturations (e.g. *SS* = 0.59% and *SS* = 0.47%) is very similar such that experimental uncertainties can explain deviations from the expected symmetry, always bearing in mind that these sensitivity curves are based on experimental size distribution and CCN data acquired at slightly different times for different *SS*.

From this sensitivity analysis we can conclude that a change in the chemical composition has only a small influence on the predicted CCN number concentrations except for very low *SS*. Since the campaign mean κ value (0.34) is representative of continental sites around the globe (Andreae and Rosenfeld, 2008; Pringle et al., 2010), a similarly weak sensitivity of CCN number concentrations to chemical composition can also be expected for other continental sites. Even smaller sensitivity to chemical composition is expected for marine regions where the mean κ is higher (0.72±0.24; Andreae and Rosenfeld, 2008; Pringle et al., 2010). However, it is important to note that this might not be true for places, where the aerosol is much less hygroscopic with lower κ values as for example reported in rainforests (Gunthe et al., 2009) or occasionally also at a site in Northern Europe (Kammermann et al., 2010a).

4.7 Using HTDMA data for CCN prediction

Here we show that HTDMA data can also be used to determine the hygroscopicity parameter κ required for the CCN prediction instead of the chemical composition data. In this case information on the mixing state of the aerosol with respect to hygroscopic properties is also known (Kammermann et al., 2010a), and the Köhler curve can be extrapolated from below saturation to the supersaturated region using the κ parameterisation. A comparison of the κ parameters derived from the different instruments is shown in Fig. 9. Since the CCN number concentration is relatively insensitive to the changes in the κ parameter, the CCNC derived κ values are very noisy, and therefore 5-h running mean values are presented for all instruments. The $D_0 = 50$ nm HTDMA measurements are most suitable for comparison with the CCN measurements at *SS* = 0.59%, because the average $D_{0,\text{crit}}$ at this *SS*, inferred from number size distribution and CCN number concentration data, is ∼56 nm. Even if there is sometimes a significant difference between the CCNC (brown dotted line) and the AMS/MAAP (black line) derived κ values, the closure comparing the measured and calculated CCN number concentration worked almost perfectly. This is because the calculated CCN number concentration is relatively insensitive to the changes in the chemical composition (κ value) as it was shown in Sect. 4.6.
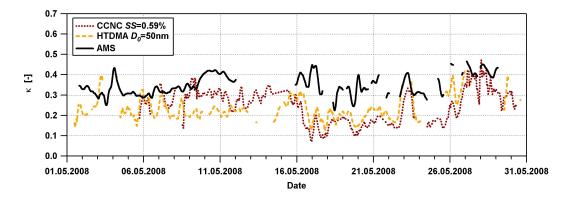
Fig. 9. Time series of hygroscopicity parameter κ derived from the different instruments.

HTDMA and CCNC derived κ values correlate well at most times and their overall agreement is better than the agreement between AMS/MAAP and CCNC derived κ values. Therefore even better agreement between CCN measurement and prediction is obtained if the size distribution data are combined with the HTDMA derived hygroscopicity parameter for the CCN prediction (not shown).

CCN predictions are complicated by several factors including the potential occurrence of surface tension suppression, bulk to surface partitioning effects of surface active species, or strong dependence of the water activity coefficient on the concentration of the solution droplet. Good et al. (2010b) reported that experimental differences between HTDMA instruments operated in parallel made it impossible to determine whether or not the above effects occur. Furthermore, CCN properties predicted from the hygroscopic growth measured at subsaturated RH were substantially different when using data from different HTDMA instruments. What does this mean for the interpretation of our closure results? Good et al. (2010b) investigated pure organic and organic dominated aerosols (organic fraction >80% for the most part) produced in a smogchamber by photo-oxidation of α-pinene. Duplissy et al. (2009) reported for this particular aerosol type discrepancies between different HTDMA instruments that compared well for inorganic aerosol during the same intercomparison study. Whether or not such discrepancies between different HTDMA instruments also occur for ambient aerosols has not yet been shown to our knowledge. The organic aerosol investigated by Good et al. (2010b) has a rather low hygroscopicity ($\kappa \sim 0.1$–0.15), which makes predicted CCN properties much more sensitive to experimental uncertainties (see Fig. 8), compared to the aerosol at the Jungfraujoch. Furthermore, the study by Good et al. (2010b) compares the properties of CCN rather than CCN number concentration. Comparison of CCN properties emphasizes small discrepancies, whereas CCN number concentrations of a polydisperse aerosol are much less sensitive to uncertainties in κ. This fact is illustrated by Figs. 4, 8 and 9 of this study: substantial differences in κ translate only into small

differences of corresponding CCN number concentrations. As a consequence it is not possible to attribute the differences in κ values reported here (Fig. 9) to experimental uncertainties or one of the above-mentioned effects with certainty, but we can constrain the hygroscopicity parameter κ from either AMS/MAAP or HTDMA measurements well enough to predict the CCN number concentration within a few percent.

4.8 Influence of Saharan dust events on the CCN number concentration

During SDE periods at the JFJ significant mass of mineral dust, predominately located in the coarse mode, might be present. Therefore it is in principle possible that the bulk chemical composition changes to that extent that our CCN predictions, which ignore mineral dust in the composition, become significantly biased. Through the one-month measurement campaign we detected only one SDE according to the criterion by Collaud Coen et al. (2004). The event was strong and lasted almost 3 days (26 May 2009 12:00–29 May 2009 12:00, CET=UTC+1). Based on previous HTDMA measurements at this site (Sjogren et al., 2008) we can state that a substantial fraction of externally mixed SDE particles can occasionally be found at $D=250$ nm in extreme cases, though a more comprehensive data set shows that the overall contribution of mineral dust at sizes with $D<265$ nm remains negligible even during strong SDE (Kammermann et al., 2010b). Here we tested the hypothesis whether neglecting mineral dust in the composition impairs our CCN prediction during the SDE or not. Therefore we split the measurement data into non-SDE and SDE periods according to the criterion by Collaud Coen et al. (2004) and compared the prediction performance between these two cases (Fig. 10). Both fitted slopes (orthogonal regression with weighting as previously explained) of 1.04 and 1.05 as well as correlation coefficients $R^2=0.99$ and 0.96 are equal within uncertainty for the non-SDE and SDE periods, respectively.
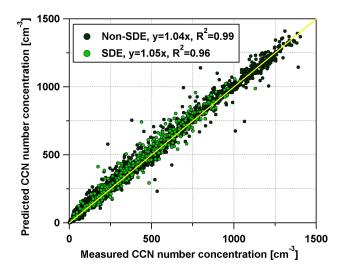
Fig. 10. Predicted vs. measured CCN number concentration during non-SDE period (dark green) and the SDE period (light green). All supersaturations are included. The yellow line represents the one-to-one ratio.

This shows that ignoring the mineral dust component in the chemical composition does not impair CCN prediction. On the contrary, using bulk composition including mineral dust would bias CCN predictions, because coarse mode mineral dust gives a major contribution to total mass (Cozic et al., 2008), whereas the contribution of mineral dust to particle number concentration at those Aitken and accumulation mode sizes in the CCN cut-off range is negligible.

5   Conclusions

The CCN number concentration observed at the Jungfraujoch was predicted reliably from measured aerosol number size distribution and chemical composition data using a simplified parameterisation of the Köhler theory. Both, average values and temporal variability of CCN number concentration were well predicted across the whole SS range. Significant underprediction was not experienced, indicating that one can assume surface tension of pure water. A comparison of HTDMA, AMS/MAAP and CCNC derived κ values showed that HTDMA measurements can be used to determine particle hygrscopicity required for CCN predictions if no suitable chemical composition measurement is available.

The composition derived campaign mean κ value was found to be $\sim$0.34. A detailed sensitivity analysis showed that this κ value is in a range, where a variation in the κ value around its mean value has only a small influence on the resulting CCN number concentration. Therefore it can be expected that the CCN number concentration at the Jungfraujoch site can generally be well predicted from size distribution data with assuming a surface tension of pure water and a constant hygroscopicity parameter of $\sim$0.34, though our
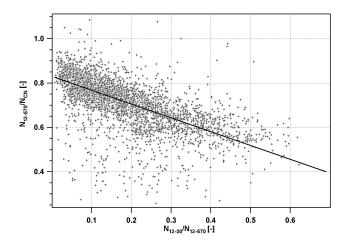

Fig. A1. The ratio between the integrated SMPS concentration (N_{12-570}) and the total concentration (N_{CN}) as a function of the fraction of small particles. The black line represents the linear fit through the data points.

long-term measurements might provide a statistically more representative value for the mean κ value. A continuous 17-months dataset with CCN number concentration and size distribution measurements will make us also able to investigate the influence of seasonal and short-term variations of the size distribution on the CCN activation at JFJ in more detail.

Appendix A

The total number concentration of particles with diameter larger than 10 nm (N_{CN}) measured by the CPC was compared to the integrated SMPS number concentration (N_{12-570}) in order to validate the SMPS measurement. The measured total number concentration is expected to be higher than N_{12-570} always if nucleation mode particles with sizes $D \approx 10$ nm are present because the CPC has a lower cut-off than the SMPS. N_{12-570} and (N_{CN}) are only expected to agree if no nucleation mode particles nor a substantial number fraction of particles with $D > 570$ nm are present. In this case any disagreement between N_{12-570} and N_{CN} is related to instrumental/measurement errors and can be used for a correction.

In Sect. 4.1 we have seen that the number concentration above 570 nm was negligible during the whole campaign, therefore we only have to exclude periods with nucleation mode particles for the comparison. In order to do so the number fraction of small particles (integrated SMPS number concentration between $D = 12$ and 30 nm, N_{12-30}) relative to total N_{12-570} was calculated as an indicator for the presence of the small particles. Then the ratio of N_{12-570} to (N_{CN}) was plotted against the proxy of the small particles (Fig. A1). As expected the ratio (N_{12-570}/N_{CN}) decreases with increasing number fraction of small particles. However, the intercept between fitted line and ordinate, i.e. the

ratio (N_{12-570}/N_{CN}) in the absence of small particles is at 0.83 instead of unity, indicating that the SMPS was undercounting by $\sim$17%. Undercounting of the SMPS may have been caused by slight deviations of the sample and sheath flow rates from the nominal values, or a DMA transfer probability which was lower than assumed. Therefore the number concentration measured by the SMPS was corrected by a size-independent factor $1/0.83 \approx 1.20$. The necessity and the absolute value of the correction factor to be applied to the SMPS data were confirmed by comparison of the measured and calculated aerosol scattering coefficient (Mie calculations using SMPS data compared to the nephelometer measurement; Fierz-Schmidhauser et al., 2010).

References

Albrecht, B. A.: Aerosols, cloud microphysics, and fractional cloudiness, Science, 245, 1227–1230, 1989.

Andreae, M. O. and Rosenfeld, D.: Aerosol-cloud-precipitation interactions. Part 1. The nature and sources of cloud-active aerosols, Earth. Sci. Rev., 89(1–2), 13–41, doi:10.1016/j.earscirev.2008.03.001, 2008.

Baltensperger, U., Gäggeler, H. W., Jost, D. T., Lugauer, M., Schwikowski, M., Weingartner, E., and Seibert, P.: Aerosol climatology at the high-alpine site Jungfraujoch, Switzerland, J. Geophys. Res., 102, 19707–19715, 1997.

Bougiatioti, A., Fountoukis, C., Kalivitis, N., Pandis, S. N., Nenes, A., and Mihalopoulos, N.: Cloud condensation nuclei measurements in the marine boundary layer of the Eastern Mediterranean: CCN closure and droplet growth kinetics, Atmos. Chem. Phys., 9, 7053–7066, doi:10.5194/acp-9-7053-2009, 2009.

Broekhuizen, K., Chang, R. Y.-W., Leaitch, W. R., Li, S.-M., and Abbatt, J. P. D.: Closure between measured and modeled cloud condensation nuclei (CCN) using size-resolved aerosol compositions in downtown Toronto, Atmos. Chem. Phys., 6, 2513–2524, doi:10.5194/acp-6-2513-2006, 2006.

Canagaratna, M. R., Jayne, J. T., Jimenez, J. L., Allan, J. D., Alfarra, M. R., Zhang, Q., Onasch, T. B., Drewnick, F., Coe, H., Middlebrook, A., Delia, A., Williams, L. R., Trimborn, A. M., Northway, M. J., DeCarlo, P. F., Kolb, C. E., Davidovits, P., and Worsnop, D. R.: Chemical and microphysical characterization of ambient aerosols with the aerodyne aerosol mass spectrometer, Mass Spec. Rev., 26, 185–222, 2007.

Clegg, S. L., Brimblecombe, P., and Wexler, A. S.: Thermodynamic model of the system $H^+-NH_4^+-Na^+-SO_4^{2-}-NO_3^--Cl^--H_2O$ at 298.15 K, J. Phys. Chem., A102, 2155–2171, 1998.

Collaud Coen, M., Weingartner, E., Nyeki, S., Cozic, J., Henning, S., Verheggen, B., Gehrig, R., and Baltensperger, U.: Long-term trend analysis of aerosol variables at the high-alpine site Jungfraujoch, J. Geophys. Res., 112, D13213, doi:10.1029/2006JD007995, 2007.

Collaud Coen, M., Weingartner, E., Schaub, D., Hueglin, C., Corrigan, C., Henning, S., Schwikowski, M., and Baltensperger, U.: Saharan dust events at the Jungfraujoch: detection by wavelength dependence of the single scattering albedo and first climatology analysis, Atmos. Chem. Phys., 4, 2465–2480, doi:10.5194/acp-4-2465-2004, 2004.

Cozic, J., Verheggen, B., Weingartner, E., Crosier, J., Bower, K. N., Flynn, M., Coe, H., Henning, S., Steinbacher, M., Henne, S., Collaud Coen, M., Petzold, A., and Baltensperger, U.: Chemical composition of free tropospheric aerosol for PM1 and coarse mode at the high alpine site Jungfraujoch, Atmos. Chem. Phys., 8, 407–423, doi:10.5194/acp-8-407-2008, 2008.

Cross, E. S., Slowik, J. G., Davidovits, P., Allan, J. D., Worsnop, D. R., Jayne, J. T., Lewis, D. K., Canagaratna, M., and Onasch, T. B.: Laboratory and ambient particle density determinations using light scattering in conjunction with aerosol mass spectrometry, Aerosol Sci. Technol., 41, 343–359, 2007.

Cubison, M. J., Ervens, B., Feingold, G., Docherty, K. S., Ulbrich, I. M., Shields, L., Prather, K., Hering, S., and Jimenez, J. L.: The influence of chemical composition and mixing state of Los Angeles urban aerosol on CCN number and cloud properties, Atmos. Chem. Phys., 8, 5649–5667, doi:10.5194/acp-8-5649-2008, 2008.

DeCarlo, P. F., Kimmel, J. R., Trimborn, A., Northway, M. J., Jayne, J. T., Aiken, A. C., Gonin, M., Fuhrer, K., Horvath, T., Docherty, K. S., Worsnop, D. R., and Jimenez, J. L.: Field-deployable, high-resolution, time-of-flight aerosol mass spectrometer, Anal. Chem., 78, 8281–8289, 2006.

Duplissy, J., Gysel, M., Sjogren, S., Meyer, N., Good, N., Kammermann, L., Michaud, V., Weigel, R., Martins dos Santos, S., Gruening, C., Villani, P., Laj, P., Sellegri, K., Metzger, A., McFiggans, G. B., Wehrle, G., Richter, R., Dommen, J., Ristovski, Z., Baltensperger, U., and Weingartner, E.: Intercomparison study of six HTDMAs: results and recommendations, Atmos. Meas. Tech., 2, 363–378, doi:10.5194/amt-2-363-2009, 2009.

Dusek, U., Frank, G. P., Hildebrandt, L., Curtius, J., Schneider, J., Walter, S., Chand, D., Drewnick, F., Hings, S., Jung, D., Borrmann, S., and Andreae, M. O.: Size matters more than chemistry for cloud-nucleating ability of aerosol particles, Science, 312, 1375–1378, 2006.

Ervens, B., Cubison, M., Andrews, E., Feingold, G., Ogren, J. A., Jimenez, J. L., DeCarlo, P., and Nenes, A.: Prediction of cloud condensation nucleus number concentration using measurements of aerosol size distributions and composition and light scattering enhancement due to humidity. J. Geophys. Res., 112, D10S32, doi:10.1029/2006JD007426, 2007.

Ervens, B., Cubison, M. J., Andrews, E., Feingold, G., Ogren, J. A., Jimenez, J. L., Quinn, P. K., Bates, T. S., Wang, J., Zhang, Q., Coe, H., Flynn, M., and Allan, J. D.: CCN predictions using simplified assumptions of organic aerosol composition and mixing state: a synthesis from six different locations, Atmos. Chem. Phys., 10, 4795–4807, doi:10.5194/acp-10-4795-2010, 2010.

Fierz-Schmidhauser, R., Zieger, P., Gysel, M., Kammermann, L., DeCarlo, P. F., Baltensperger, U., and Weingartner, E.: Measured and predicted aerosol light scattering enhancement factors at the high alpine site Jungfraujoch, Atmos. Chem. Phys., 10, 2319–2333, doi:10.5194/acp-10-2319-2010, 2010.

Good, N., Topping, D. O., Allan, J. D., Flynn, M., Fuentes, E., Irwin, M., Williams, P. I., Coe, H., and McFiggans, G.: Consistency between parameterisations of aerosol hygroscopicity and CCN activity during the RHaMBLe discovery cruise, Atmos. Chem. Phys., 10, 3189–3203, doi:10.5194/acp-10-3189-2010, 2010a.

Good, N., Topping, D. O., Duplissy, J., Gysel, M., Meyer, N. K., Metzger, A., Turner, S. F., Baltensperger, U., Ristovski, Z., Weingartner, E., Coe, H., and McFiggans, G.: Widening the gap between measurement and modelling of secondary organic aerosol properties?, Atmos. Chem. Phys., 10, 2577–2593, doi:10.5194/acp-10-2577-2010, 2010b.

Gunthe, S. S., King, S. M., Rose, D., Chen, Q., Roldin, P., Farmer, D. K., Jimenez, J. L., Artaxo, P., Andreae, M. O., Martin, S. T., and Pöschl, U.: Cloud condensation nuclei in pristine tropical rainforest air of Amazonia: size-resolved measurements and modeling of atmospheric aerosol composition and CCN activity, Atmos. Chem. Phys., 9, 7551–7575, doi:10.5194/acp-9-7551-2009, 2009.

Gysel, M., McFiggans, G. B., and Coe, H.: Inversion of tandem differential mobility analyser (TDMA) measurements, J. Aerosol Sci., 40, 134–151, 2009.

Henning, S., Weingartner, E., Schmidt, S., Wendisch, M., Gäggeler, H. W., and Baltensperger, U.: Size-dependent aerosol activation at the high-alpine site Jungfraujoch (3580 m asl), Tellus, 54B, 82–95, 2002.

Henning, S., Weingartner, E., Schwikowski, M., Gäggeler, H. W., Gehrig, R., Hinz, K. P., Trimborn, A., Spengler, B., and Baltensperger, U.: Seasonal variation of water-soluble ions of the aerosol at the high-alpine site Jungfraujoch (3580 m a.s.l.), J. Geophys. Res., 108, 4030, doi:10.1029/2002JD002439, 2003.

Herich, H., Tritscher, T., Wiacek, A., Gysel, M., Weingartner, E., Lohmann, U., Baltensperger, U., and Cziczo, D. J.: Water uptake of clay and desert dust aerosol particles at sub- and super-saturated water vapor conditions, Phys. Chem. Chem. Phys., 11, 7804–7809, 2009.

IPCC, Solomon, S., Qin, D., Manning, M., Marquis, M., Averyt, K., Tignor, M. M. B., Miller, H. L. J., and Chen, Z. (eds.): Climate Change 2007 – The Physical Science Basis. Contribution of Working Group I to the Fourth Assessment Report of the Intergovernmental Panel on Climate Change, Cambridge University Press, Cambridge, 153–154 and 171–172, 2007.

Jurányi, Z., Gysel, M., Duplissy, J., Weingartner, E., Tritscher, T., Dommen, J., Henning, S., Ziese, M., Kiselev, A., Stratmann, F., George, I., and Baltensperger, U.: Influence of gas-to-particle partitioning on the hygroscopic and droplet activation behaviour of α-pinene secondary organic aerosol, Phys. Chem. Chem. Phys., 11, 8091–8097, 2009.

Kammermann, L., Gysel, M., Weingartner, E., Herich, H., Cziczo, D. J., Holst, T., Svenningsson, B., Arneth, A., and Baltensperger, U.: Subarctic atmospheric aerosol composition: 3. Measured and modeled properties of cloud condensation nuclei, J. Geophys. Res., 115, D04202, doi:10.1029/2009JD012447, 2010a.

Kammermann, L., Gysel, M., Weingartner, E., and Baltensperger,

U.: 13-month climatology of the aerosol hygroscopicity at the free tropospheric site Jungfraujoch (3580 m a.s.l.), Atmos. Chem. Phys. Discuss., 10, 13573–13608, doi:10.5194/acpd-10-13573-2010, 2010b.

Keith, C. H. and Arons, A. B.: The growth of sea-salt particles by condensation of atmospheric water vapor. J. Meteorol., 11, 173–184, 1954.

King, S. M., Rosenoern, T., Shilling, J. E., Chen, Q., and Martin, S. T.: Increased cloud activation potential of secondary organic aerosol for atmospheric mass loadings, Atmos. Chem. Phys., 9, 2959–2971, doi:10.5194/acp-9-2959-2009, 2009.

Koehler, K. A., Kreidenweis, S. M., DeMott, P. J., Petters, M. D., Prenni, A. J., and Carrico, C. M.: Hygroscopicity and cloud droplet activation of mineral dust aerosol. Geophys. Res. Lett., 36, L08805, doi:10.1029/2009GL037348, 2009.

Köhler, H.: The nucleus in and the growth of hygroscopic droplets. Trans. Faraday Soc., 32, 1152–1161, 1936.

Krivácsy, Z., Hoffer, A., Sárvári, Z., Temesi, D., Baltensperger, U., Nyeki, S., Weingartner, E., Kleefeld, S., and Jennings, S. G.: Role of organic and black carbon in the chemical composition of atmospheric aerosol at European background sites, Atmos. Environ., 35, 6231–6244, 2001.

Kulmala, M., Asmi, A., Lappalainen, H. K., Carslaw, K. S., Pöschl, U., Baltensperger, U., Hov, Ø., Brenquier, J.-L., Pandis, S. N., Facchini, M. C., Hansson, H.-C., Wiedensohler, A., and O'Dowd, C. D.: Introduction: European Integrated Project on Aerosol Cloud Climate and Air Quality interactions (EUCAARI) – integrating aerosol research from nano to global scales, Atmos. Chem. Phys., 9, 2825–2841, doi:10.5194/acp-9-2825-2009, 2009.

Kuwata, M., Kondo, Y., and Takegawa, N.: Critical condensed mass for activation of black carbon as cloud condensation nuclei in Tokyo, J. Geophys. Res., 114, D20202, doi:10.1029/2009JD012086, 2009.

Lance, S., Nenes, A., Mazzoleni, C., Dubey, M. K., Gates, H., Varutbangkul, V., Rissman, T. A., Murphy, S. M., Sorooshian, A., Flagan, R. C., Seinfeld, J. H., Feingold, G., and Jonsson, H. H.: Cloud condensation nuclei activity, closure, and droplet growth kinetics of Houston aerosol during the Gulf of Mexico Atmospheric Composition and Climate Study (GoMACCS), J. Geophys. Res., 114, D00F15, doi:10.1029/2008JD011699, 2009.

Liu, P. S. K., Leaitch, W. R., Banic, C. M., Li, S. M., Ngo, D., and Megaw, W. J.: Aerosol observations at Chebogue Point during the 1993 North Atlantic Regional Experiment: Relationships among cloud condensation nuclei, size distribution, and chemistry, J. Geophys. Res., 101, 28971–28990, 1996.

McFiggans, G., Artaxo, P., Baltensperger, U., Coe, H., Facchini, M. C., Feingold, G., Fuzzi, S., Gysel, M., Laaksonen, A., Lohmann, U., Mentel, T. F., Murphy, D. M., O'Dowd, C. D., Snider, J. R., and Weingartner, E.: The effect of physical and chemical aerosol properties on warm cloud droplet activation, Atmos. Chem. Phys., 6, 2593–2649, doi:10.5194/acp-6-2593-2006, 2006.

Moore, R. H., Ingall, E. D., Sorooshian, A., and Nenes, A.: Molar mass, surface tension, and droplet growth kinetics of marine organics from measurements of CCN activity, Geophys. Res. Lett., 35, L07801, doi:10.1029/2008GL033350, 2008.

Nyeki, S., Baltensperger, U., Colbeck, I., Jost, D. T., Weingart-

ner, E., and Gäggeler, H. W.: The Jungfraujoch high-Alpine research station (3454 m) as a background clean continental site for the measurement of aerosol parameters, J. Geophys. Res., 103, 6097–6107, 1998.

Park, K., Kittelson, D., and McMurry, P.: Structural properties of diesel exhaust particles measured by transmission electron microscopy (TEM): relationships to particle mass and mobility, Aerosol Sci. Technol., 38, 881–889, 2004.

Petters, M. D. and Kreidenweis, S. M.: A single parameter representation of hygroscopic growth and cloud condensation nucleus activity, Atmos. Chem. Phys., 7, 1961–1971, doi:10.5194/acp-7-1961-2007, 2007.

Petters, M. D. and Kreidenweis, S. M.: A single parameter representation of hygroscopic growth and cloud condensation nucleus activity – Part 2: Including solubility, Atmos. Chem. Phys., 8, 6273–6279, doi:10.5194/acp-8-6273-2008, 2008.

Petzold, A. and Schonlinner, M.: Multi-angle absorption photometry – a new method for the measurement of aerosol light absorption and atmospheric black carbon. J. Aerosol Sci., 35, 421–441, 2004.

Petzold, A., Schloesser, H., Sheridan, P. J., Arnott, W. P., Ogren, J. A., and Virkkula, A.: Evaluation of multiangle absorption photometry for measuring aerosol light absorption. Aerosol Sci. Technol., 39, 40–51, 2005.

Pringle, K. J., Tost, H., Pozzer, A., Pöschl, U., and Lelieveld, J.: Global distribution of the effective aerosol hygroscopicity parameter for CCN activation, Atmos. Chem. Phys., 10, 5241–5255, doi:10.5194/acp-10-5241-2010, 2010.

Roberts, G. C. and Nenes, A.: A continuous-flow streamwise thermal-gradient CCN chamber for atmospheric measurements, Aerosol Sci. Technol., 39, 206–221, 2005.

Rose, D., Gunthe, S. S., Mikhailov, E., Frank, G. P., Dusek, U., Andreae, M. O., and Pöschl, U.: Calibration and measurement uncertainties of a continuous-flow cloud condensation nuclei counter (DMT-CCNC): CCN activation of ammonium sulfate and sodium chloride aerosol particles in theory and experiment, Atmos. Chem. Phys., 8, 1153–1179, doi:10.5194/acp-8-1153-2008, 2008.

Saxena, P. and Hildemann, L. M.: Water-soluble organics in atmospheric particles: A critical review of the literature and application of thermodynamics to identify candidate compounds, J. Atmos. Chem., 24, 57–109, 1996.

Shilling, J. E., King, S. M., Mochida, M., Worsnop, D. R., and Martin, S. T.: Mass spectral evidence that small changes in composition caused by oxidative aging processes alter aerosol CCN properties, J. Phys. Chem. A, 111 (17), 3358–3368, 2007.

Shulman, M. L., Jacobson, M. C., Carlson, R. J., Synovec, R. E., and Young, T. E.: Dissolution behavior and surface tension effects of organic compounds in nucleating cloud droplets, Geophys. Res. Lett., 23, 277–280, 1996.

Sjogren, S., Gysel, M., Weingartner, E., Alfarra, M. R., Duplissy, J., Cozic, J., Crosier, J., Coe, H., and Baltensperger, U.: Hygroscopicity of the submicrometer aerosol at the high-alpine site Jungfraujoch, 3580 m a.s.l., Switzerland, Atmos. Chem. Phys., 8, 5715–5729, doi:10.5194/acp-8-5715-2008, 2008.

Sjogren, S., Gysel, M., Weingartner, E., Baltensperger, U., Cubison, M. J., Coe, H., Zardini, A., Marcolli, C., Krieger, U. K., and Peter, T.: Hygroscopic growth and water uptake kinetics of two-phase aerosol particles consisting of ammonium sulfate, adipic and humic acid mixtures, J. Aerosol Sci., 38, 157–171, 2007.

Sorjamaa, R., Svenningsson, B., Raatikainen, T., Henning, S., Bilde, M., and Laaksonen, A.: The role of surfactants in Köhler theory reconsidered, Atmos. Chem. Phys., 4, 2107–2117, doi:10.5194/acp-4-2107-2004, 2004.

Stokes, R. H. and Robinson, R. A.: Interactions in aqueous nonelectrolyte solutions. I. Solute-solvent equilibria, J. Phys. Chem., 70, 2126–2130, 1966.

Stroud, C. A., Nenes, A., Jimenez, J. L., DeCarlo, P. F., Huffman, J. A., Bruintjes, R., Nemitz, E., Delia, A. E., Toohey, D. W., Guenther, A. B., and Nandi, S.: Cloud activating properties of aerosol observed during CELTIC, J. Atmos. Sci., 64, 441–459, 2007.

Topping, D. O., McFiggans, G. B., and Coe, H.: A curved multi-component aerosol hygroscopicity model framework: Part 1 – Inorganic compounds, Atmos. Chem. Phys., 5, 1205–1222, doi:10.5194/acp-5-1205-2005, 2005.

Twomey, S.: Influence of pollution on shortwave albedo of clouds, J. Atmos. Sci., 34, 1149–1152, 1977.

Vestin, A., Rissler, J., Swietlicki, E., Frank, G. P., and Andreae, M. O.: Cloud-nucleating properties of the Amazonian biomass burning aerosol: Cloud condensation nuclei measurements and modeling, J. Geophys. Res., 112, D14201, doi:10.1029/2006JD8104, 2007

Weingartner, E., Burtscher, H., and Baltensperger, U.: Hygroscopic properties of carbon and diesel soot particles, Atmos. Environ., 31, 2311–2327, 1997.

Weingartner, E., Nyeki, S., and Baltensperger, U.: Seasonal and diurnal variation of aerosol size distributions (10<D<750nm) at a high-alpine site (Jungfraujoch 3580 m asl), J. Geophys. Res., 104, 26809–26820, 1999.

Weingartner, E., Gysel, M., and Baltensperger, U.: Hygroscopicity of aerosol particles at low temperatures. 1. New low-temperature H-TDMA instrument: Setup and first applications, Environ. Sci. Technol., 36, 55–62, 2002.

Zhang, Q., Jimenez, J. L., Canagaratna, M. R., Allan, J. D., Coe, H., Ulbrich, I., Alfarra, M. R., Takami, A., Middlebrook, A. M., Sun, Y. L., Dzepina, K., Dunlea, E., Docherty, K., DeCarlo, P. F., Salcedo, D., Onasch, T., Jayne, J. T., Miyoshi, T., Shimono, A., Hatakeyama, S., Takegawa, N., Kondo, Y., Schneider, J., Drewnick, F., Borrmann, S., Weimer, S., Demerjian, K., Williams, P., Bower, K., Bahreini, R., Cottrell, L., Griffin, R. J., Rautiainen, J., Sun, J. Y., Zhang, Y. M., and Worsnop, D. R.: Ubiquity and dominance of oxygenated species in organic aerosols in anthropogenically-influenced Northern Hemisphere midlatitudes, Geophys. Res. Lett., 34, L13801, doi:10.1029/2007GL029979, 2007.